sequencing on an Illumina NovaSeq 6000 platform. Raw sequencing data underwent quality control to remove adapter sequences and low-quality reads, yielding high-quality clean reads, which were then mapped to the K955 reference genome using HISAT2. Gene-function annotation was performed using the Nr, Nt, Pfam, KOG/COG, Swiss-Prot, KO, and GO databases. Differential expression genes (DEGs) analysis was performed using DESeq2 R (v1.26.0), with statistical significance defined as $|\log_2\text{Fold Change}| > 1$ and adjusted p-value < 0.05. Gene Ontology (GO) function-enrichment analysis and Kyoto Encyclopedia of Genes and Genomes (KEGG) pathway-enrichment analysis of DEGs were performed using Goatools and KOBAS software, respectively.

### 2.7 Analytical methods

Quantitative determination of glucose and D-arabitol was performed using a Dionex UltiMate 3000 high-performance liquid chromatography system equipped with a Corona Charged Aerosol Detector (CAD). Chromatographic separation was achieved using an Aminex HPX-87H (Φ 7.8 mm × 300 mm) with 5 mM $H_2SO_4$ as the mobile phase at a flow rate of 0.6 mL/min and a column temperature of 65°C. Under these conditions, glucose, D-arabitol, and glycerol were eluted at retention times of 8.8, 10.6, and 13.0 min, respectively.

For measurement of intracellular ATP, ROS levels, and NADPH contents, we collected samples at 156 h of fermentation. Intracellular ATP content was determined using an ATP assay kit (Solarbio, China) based on the hexokinase (HK) method. Intracellular NADPH content was measured using an NADPH assay kit (Solarbio, China). Intracellular reactive oxygen species (ROS) levels were detected using the fluorescent probe dihydroethidium (DHE) (Beyotime, China). Fluorescence intensity was recorded at an excitation wavelength of 535 nm and an emission wavelength of 610 nm, and relative ROS levels were expressed as the ratio of fluorescence intensity to $OD_{600}$. Total protein concentration used for normalizing the above biochemical parameters was determined using a BCA protein-assay kit (Solarbio, China) with bovine serum albumin (BSA) as the standard.



### 2.8 Optimization of fermentation conditions and scaling of the fermenter

To maximize D-arabitol production by mutant strain A37, we first investigated the optimal substrate concentration for A37. Next, under optimal substrate conditions, we systematically optimized the fermentation parameters for A37. Single-factor experimental design was adopted at the shake-flask scale, with a liquid volume of 30 mL in a 250 mL shake flask. The effects of nitrogen source type and concentration, inorganic ions, culture temperature, and initial pH on product synthesis were examined. Temperature was evaluated across a range of 26-34℃, pH across a range of 2-8, and inorganic ion concentration at 5 mM. Yeast extract from various sources was tested as the nitrogen source at a final concentration ranging from 5 g/L to 20 g/L.

Fed-batch fermentation validation of mutant strain A37 was conducted in a 3L bioreactor with a working volume of 2 L. Culture pH was maintained at 4.0 by automatic addition of ammonia water. Temperature was held at 30℃, and aeration was set at 1.5 vvm. Dissolved oxygen (DO) was controlled at 25% through cascade stirring ranging from 400 to 1000 rpm. To maintain a hyperosmotic environment and ensure continuous substrate availability, a concentrated glucose solution (900 g/L) was fed when residual glucose concentration fell below 80 g/L, maintaining an approximate glucose concentration of 230 g/L in the culture broth. Samples were collected at regular time intervals during fermentation to measure cell density, residual glucose concentration, and D-arabitol titer.

## 3 Results

### 3.1 Screening and identification of high D-arabitol-producing yeast strains

To isolate a robust strain for D-arabitol production, we screened a library consisting of 68 osmotolerant

yeast isolates from our collection. Most strains exhibited favorable growth characteristics in high-glucose medium. Based on the primary screening results, we selected six representative strains that displayed the highest potential for distinct quantification of metabolite profiles (Fig.S1). Strain K955 demonstrated the highest production potential, yielding approximately 42 g/L after 96 h of shake-flask fermentation, and was therefore selected as the wild-type chassis strain for subsequent experiments.

Phylogenetic analysis based on 18S rDNA sequencing revealed that strain K955 shared 99% sequence homology with the type strains *W. anomalus* Y-161 and *W. subpelliculosus* NRRL Y-1683 (Fig.S2). Whole-genome sequencing confirmed the strain's identification as *W. anomalus*. The complete genome sequence has been deposited in the NCBI GenBank database (accession number JBQYEW000000000). The assembled genome (Fig.S3) spanned approximately 13.83 Mb with a GC content of 32.04%. Genome annotation identified 5,306 protein-coding genes, representing 57.73% of the total genome size. Following assembly and quality assessment, GC content distribution ranged primarily between 30% and 50%, with sequencing depth concentrated in the range of 30~300×. The majority of predicted genes (721 Unigenes, ~13.59%) exhibited lengths ≥2500 bp.

KEGG pathway annotation revealed that K955 genes were extensively involved in carbon metabolism, amino acid metabolism, and secondary-metabolite synthesis pathways (Fig.S4), indicating an active primary metabolic network that supports robust cellular function. GO function annotation further demonstrated that gene functions were predominantly enriched in core biological processes, molecular functions, and cellular components (Fig.S5), which are essential for maintaining normal yeast metabolism. Collectively, the genomic analysis confirmed the presence of a complete metabolic framework such as required for substrate conversion, thereby providing the genetic basis necessary for efficient D-arabitol biosynthesis.

### 3.2 Optimization of initial glucose concentration for D-arabitol production by K955

Establishing optimal fermentation conditions is essential for enabling industrial application of a strain. The influence of initial glucose concentration on D-arabitol production by K955 was systematically evaluated, and the results revealed a positive correlation between production capacity and substrate tolerance, though an optimal threshold existed. At glucose concentrations below 350 g/L, premature substrate depletion led cells to catabolize the accumulated product during the late fermentation stage, thereby reducing the final D-arabitol titer (Fig.1a). At 350 g/L, K955 achieved a maximum titer of 88.75 g/L at 156 h with complete glucose consumption (Fig.1b). At this concentration, HPLC analysis also detected the accumulation of glycerol, a common compatible solute produced by yeast to counteract osmotic stress(Blomberg and Adler, 1992). However, when the initial glucose concentration was elevated to 400 g/L, cell growth and product formation were markedly inhibited, and substrate utilization decreased to approximately 50% over the same fermentation period. High substrate concentrations induce yeast cells to synthesize and accumulate D-arabitol intracellularly to balance osmotic pressure across the cell membrane and prevent dehydration(Blomberg and Adler, 1992), but the product remains largely confined within the cells, resulting in a slower increase in extracellular D-arabitol levels. Based on these observations, 350 g/L was identified as the optimal initial glucose concentration for K955. These results underscore the substrate-inhibition challenge faced by the wild-type strain at elevated glucose concentrations and provide a clear rationale for subsequent mutagenesis efforts aimed at isolating mutants with enhanced osmotic tolerance.

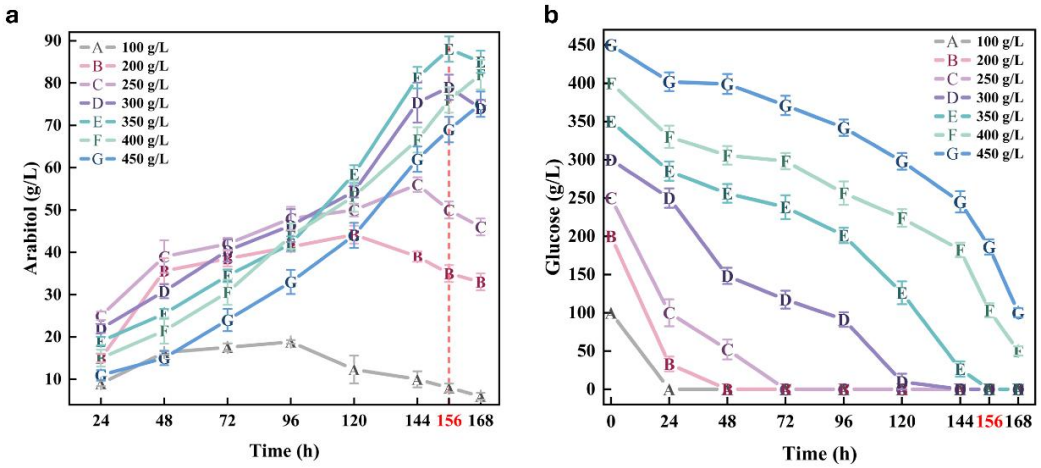


**Fig. 1 Screening and identification of *W. anomalus* K955. (a) Arabitol production by *W. anomalus* K955 at different glucose concentrations. (b) Glucose consumption by *W. anomalus* K955 at different glucose concentrations. A–G represent initial glucose concentrations of 100 g/L, 200 g/L, 250g/L, 300 g/L, 350g/L, 400g/L and 500 g/L, respectively.**

### 3.3 Isolation of high-producing mutants through combinatorial mutagenesis and INT-based colorimetric HTS

To overcome the performance limitations of the wild-type strain, we subjected K955 to low-energy $N^+$-ion implantation mutagenesis (Fig.2a). Based on a 25% survival-rate threshold(Yan et al., 2017), the implantation parameters were optimized to a dose of 100 ion·cm$^{-2}$ at an energy of 20 keV, with a preset dose of 1026 keV·$10^{13}$ion/cm$^2$ and an actual dose of 1031 keV·$10^{13}$ion/cm$^2$. This protocol generated a rich mutant library while maintaining an acceptable survival rate. Subsequently, a HTS method based on INT colorimetric analysis was established (Fig.S6).

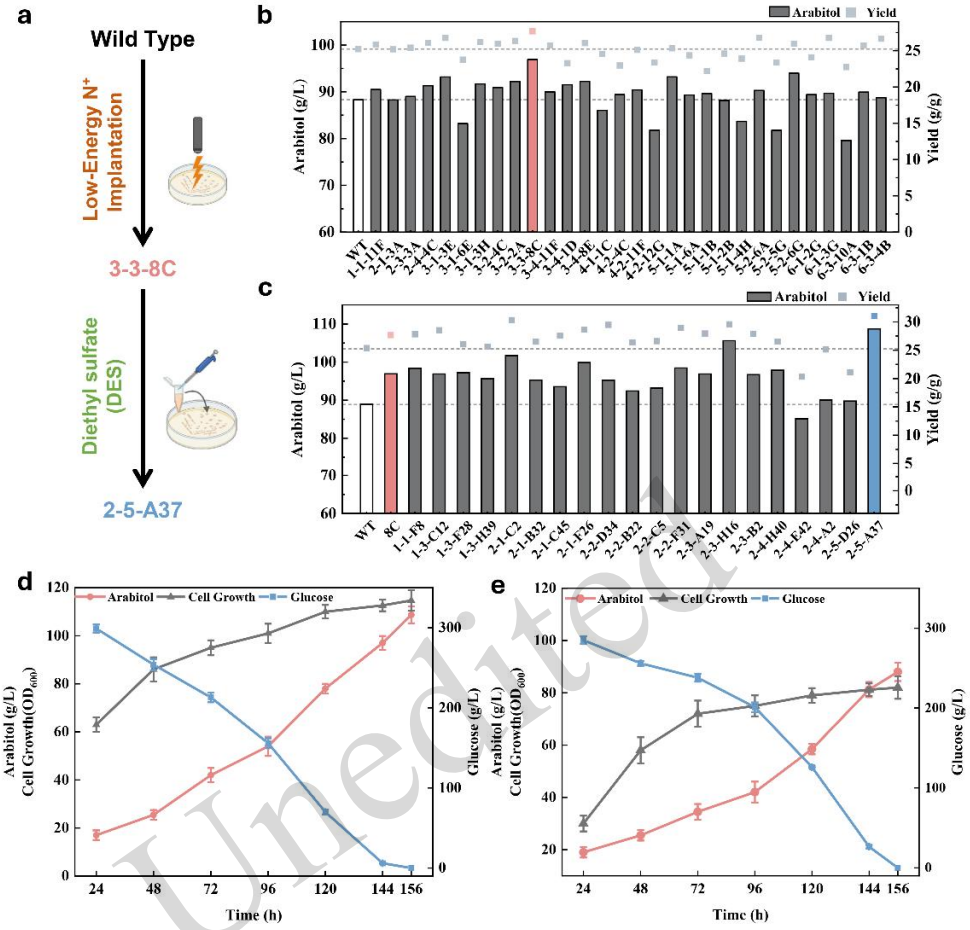


**Fig. 2 (a) Low-energy $N^+$ implantation combined with DES mutagenesis. (b) HPLC evaluation of positive mutants screened from $N^+$ ion implantation. (c)HPLC evaluation of positive mutants screened from DES mutagenesis. (d) K955 fermentation curve (e) A37 fermentation curve.**

Through HTS of approximately 2000 mutant strains, 30 candidate strains were selected for subsequent HPLC verification, from which several positive mutants with markedly improved D-arabitol production were identified. The accuracy rate of the HTS procedure (the number of positive results determined by HPLC / the number of positive results screened out by HTS) was concurrently validated, reaching approximately 70%. Notably, mutant strain 3-3-8C (8C) achieved a titer of 96.9 g/L, representing a 9.0% increase over the wild type, and a yield of 0.28 g/g, corresponding to a 10.6% improvement (Fig.2b). Secondary mutagenesis of strain 3-3-8C was subsequently performed using DES, with the optimal treatment duration determined to be 25 min, corresponding to a survival rate of approximately 25% (Fig.S7). The INT-based colorimetric HTS was then applied to the resulting mutant library, from which Strain A37 was identified as the top-performing mutant, achieving a titer of 108.69 g/L and a yield of 0.31 g/g (Fig.2c), representing 22.3% and 23.1% improvements, respectively, compared to the wild type. Crucially, the byproduct profile revealed that glycerol production in A37 increased only marginally to 15.4 g/L, compared to 14.8 g/L in the wild type. The significant increase in D-arabitol titer in contrast to the relatively stable glycerol accumulation indicates that the combinatorial mutagenesis directed the enhanced metabolic flux specifically toward the target product.

To rigorously assess the metabolic advantages of the mutant, we compared the fermentation kinetics of wild-type K955 and mutant A37 in shake flasks (Fig.2d; Fig.2e). Although the overall glucose-consumption

profiles were similar, A37 clearly exhibited higher metabolic flux, supporting faster cell proliferation. A37 reached a substantially higher cell density than K955, with the final $OD_{600}$ being approximately 1.4-fold greater than that of the parent strain, indicating that the mutations effectively alleviated growth constraints and enabled more efficient product synthesis. Driven by the increased biomass and enhanced metabolic activity, A37 attained a final D-arabitol titer of 108.69 g/L, significantly surpassing that of K955. Strain A37 maintained stable production performance over 10 successive subcultures (Fig.S8), and has been deposited in the Guangdong Microbial Culture Collection Center (GDMCC No. 65731). Recent studies have demonstrated that such accelerated evolution through ion implantation can effectively reprogram metabolic networks to enhance osmotic tolerance and metabolite production. In our study, the integration of this technique with DES treatment likely created a synergistic effect, enabling mutant A37 to bypass the natural substrate inhibition common in wild-type strains. This is consistent with the findings of Zhang(Zhang et al., 2024) and Zheng(Zheng et al., 2020), who reported that random mutagenesis, particularly when combined with transcriptomic guidance, can successfully elevate polyol biosynthesis by rebalancing intracellular redox states and precursor availability. Collectively, these results highlight the effectiveness of the combinatorial mutagenesis strategy that integrates physical mutagenesis, chemical mutagenesis, and INT-based high-throughput screening in reprogramming the metabolism of the wild-type strain and isolating high-performance candidates with clear industrial application potential.

### 3.4 Transcriptomics reveals metabolic reprogramming in mutant strain A37

To elucidate the molecular mechanism underlying the high D-arabitol titer of strain A37, comparative transcriptomic analysis (RNA-Seq) was performed for the wild-type strain K955 and the mutant A37. Principal Component Analysis (PCA) revealed clear separation between the two sample groups (Fig.S9) and sequencing quality metrics were excellent (Table.S1), indicating substantial transcriptional reprogramming induced by mutagenesis. Differential gene-expression analysis identified 656 upregulated genes and 366 downregulated genes in A37 relative to K955 ($P < 0.05$; Fig.S10, reflecting extensive remodeling of the global metabolic network.

GO and KEGG enrichment analyses revealed two critical metabolic shifts in A37 (Fig.3a&Fig.S11). First, the mutant strain substantially enhanced protein synthesis capacity and genetic fidelity, enabling effective adaptation to mutagenesis-induced stress and establishing a robust material foundation to sustain the 1.4-fold increase in biomass and high-intensity metabolism. Second, a decisive reallocation of carbon metabolic flux was evident: expression of key glycolytic enzymes in the Embden-Meyerhof-Parnas Pathway (EMP) and the PPP was upregulated in A37, whereas genes encoding catabolic enzymes for complex carbon sources (α-glucans, disaccharides, and fatty acids) were downregulated. This metabolic reprogramming reflects a cellular preference for rapid glucose catabolism through central carbon metabolism rather than diversion toward storage-compound biosynthesis. Biochemical assays corroborated this inference. Intracellular ATP levels in A37 were 67% higher than those in the wild type (Fig.3b). This elevated energy state, consistent with EMP pathway upregulation, provided sufficient thermodynamic driving force for biosynthesis while maintaining metabolic flux below the threshold for glycolytic feedback inhibition, thereby sustaining efficient metabolic equilibrium. Notably, concurrent upregulation of genes encoding key EMP and PPP enzymes, including glucose-6-phosphate dehydrogenase (*zwf*), 6-phosphogluconate dehydrogenase (*gnd*), and ribulose-5-phosphate 3-epimerase (*rpe*), was observed (Fig.3c). The PPP serves the dual function of supplying biosynthetic precursor (D-ribulose-5-phosphate) and regenerating reducing power (NADPH). Consistent with the transcriptomic data, biochemical assays demonstrated that intracellular NADPH levels in A37 were significantly elevated relative to the wild type (Fig.3b). This expanded NADPH pool served two complementary functions: first, it provided essential reducing equivalents for the D-arabitol biosynthetic reactions, driving metabolic flux toward product accumulation; second, it augmented cellular redox buffering

capacity. Although the vigorous metabolic activity of A37 inevitably generated elevated intracellular ROS levels (Fig.3b), the high NADPH availability enhanced the cell's antioxidant capacity, enabling preservation of redox homeostasis and prevention of oxidative damage under heightened ROS stress. Furthermore, we propose that this moderately elevated ROS functions not merely as a metabolic byproduct but as an endogenous signaling molecule. In synergy with osmotic stress, it further amplifies D-arabitol biosynthesis as a protective compatible solute, a mechanism analogous to ROS-mediated metabolite-accumulation strategies reported in other stress-tolerant fungi(Shi et al., 2017).

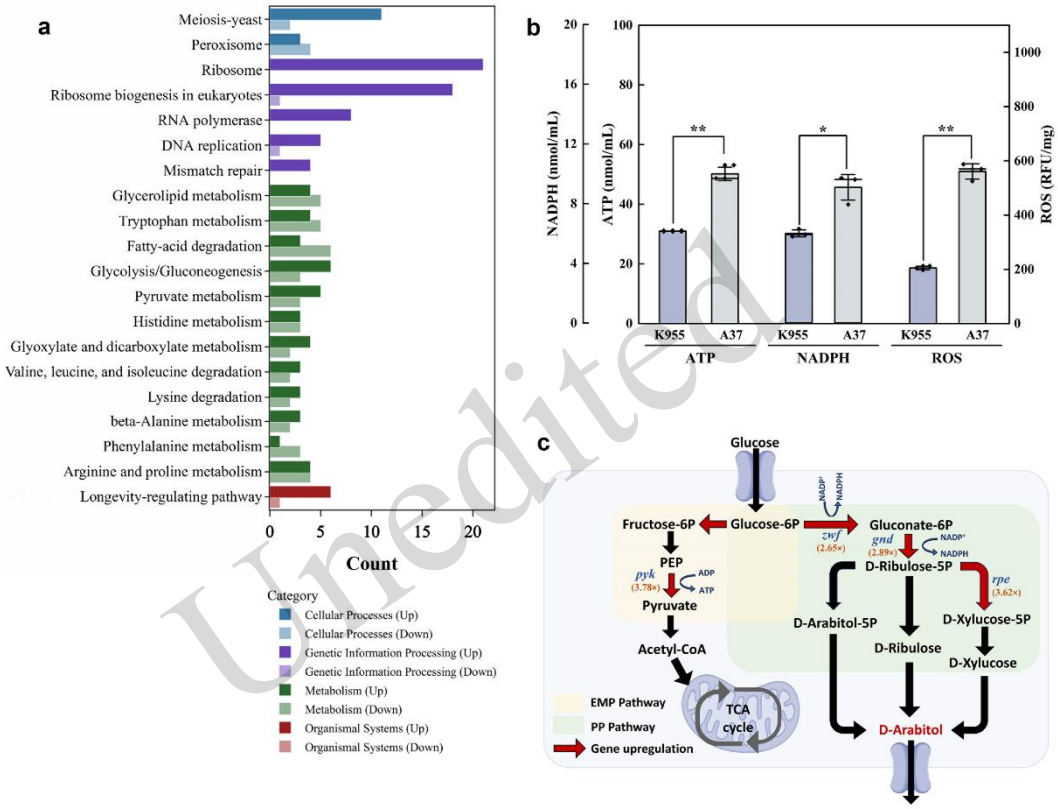


**Fig. 3 Comparative transcriptomic analysis of mutant A37 against wild-type K955. (a) KEGG-enrichment analysis of DEGs. (b) Intracellular ATP, NADPH concentration, and relative ROS levels of K955 and A37($p<0.05$). (c) Schematic diagram of genes involved in D-arabitol production pathways.**

In summary, the high-production phenotype of A37 reflects the establishment of a novel metabolic homeostasis characterized by strategic reallocation of cellular resources from maintenance metabolism toward growth and product synthesis through comprehensive metabolic reprogramming. This phenotype achieves synergistic coordination among precursor availability, which reduces power regeneration and strengthens oxidative stress defense by reinforcing PPP flux.

### 3.5 Optimization of fermentation conditions and scale-up validation of strain A37

To maximize the production potential of A37, shake-flask fermentation conditions were systematically optimized to establish key process parameters for subsequent industrial scale-up. Results revealed that the optimal substrate concentration for A37 was 400 g/L (Fig.4a), 50 g/L higher than the wild-type strain. Under these conditions, we first investigated the effects of temperature and initial pH. The results showed that strain A37 achieved maximum cell growth and D-arabitol production at 30℃ (Fig.4b), representing the optimal balance between rapid cell proliferation and efficient product accumulation. Evaluation of pH effects revealed

that A37 exhibited peak production at pH 4 (Fig.4c). To optimize the nitrogen source, yeast extracts from different suppliers—Aladdin (China; Cat# Y110517), OXOID (UK; Cat# LP0021), and Angel Yeast (China; Cat# FM888)—were evaluated. Nitrogen-source screening identified Yeast extract (Aladdin, China) as the optimal source, with maximum D-arabitol production at a final concentration of 10 g/L (Fig.4d). This variation stems from the distinct yeast strains and hydrolysis processes employed by manufacturers, which lead to substantial differences in product composition such as amino acid profiles, vitamins, cofactors, nucleotides, and minerals. Furthermore, the ratio of proteins that is degraded into small peptides versus free amino acids may vary. These differences in micro-components likely regulate the oxidative stress response and osmotic balance within the pentose phosphate pathway (PPP), leading to significant fluctuations in D-arabitol production. Assessment of inorganic salt supplementation demonstrated that most inorganic salts did not enhance the titer (Fig.4e). Consolidating these single-factor optimization results, the optimal shake-flask fermentation parameters for strain A37 were determined as follows: 30℃, initial pH 4.0, 10 g/L Yeast extract (Aladdin, China) as the nitrogen source, and no additional inorganic salts.

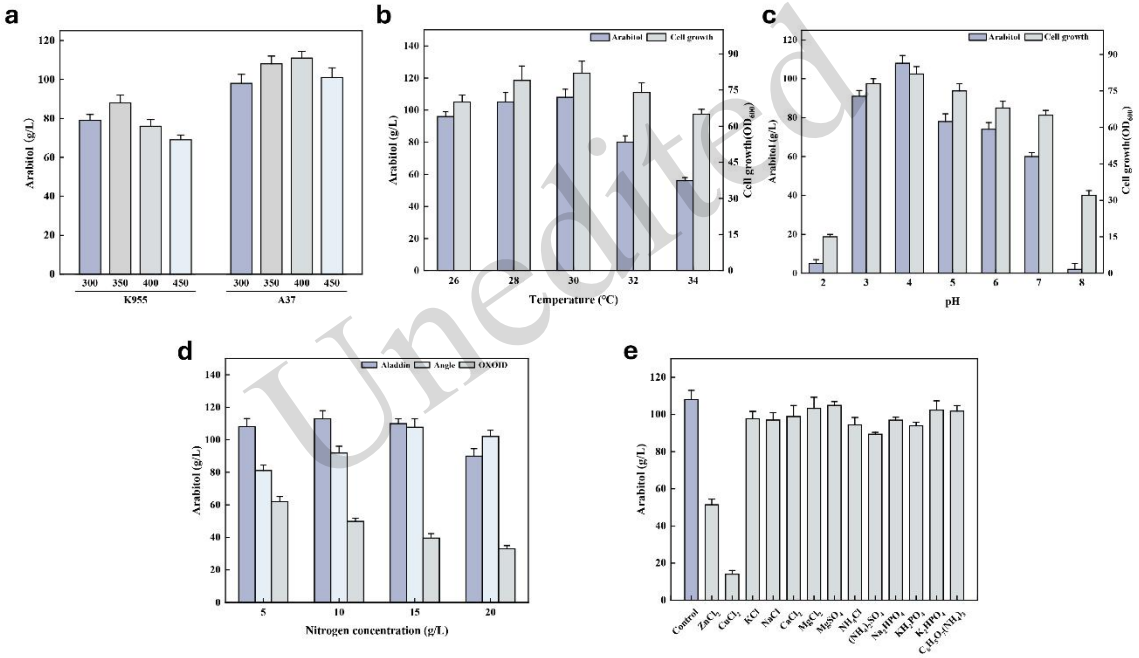


**Fig. 4 Optimization of fermentation conditions for A37. (a). Substrate concentration. (b)Temperature. (c). pH; (d). Nitrogen source. (e). Inorganic salts. Unless otherwise specified, the default fermentation conditions were: initial glucose 350 g/L, temperature 30°C, initial pH 4.0, 10 g/L yeast extract (Aladdin), and no additional inorganic salts.**

We conducted fed-batch fermentation in a 3L bioreactor to evaluate large-scale production performance of A37 under controlled conditions (Fig.5). The fermentation process exhibited three distinct phases, characterized by different metabolic priorities.

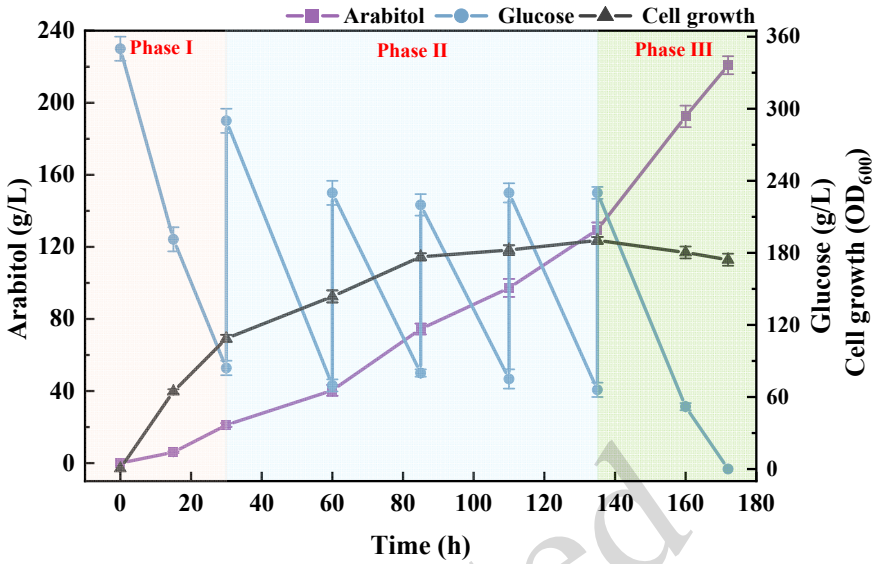


**Fig. 5 Time courses of D-arabitol production, D-glucose consumption, and biomass production during fed-batch fermentation of A37.**



Phase I (0-30 h): Rapid cell growth. During this phase, the carbon source was rapidly consumed and mainly allocated to biomass accumulation. The $OD_{600}$ reached 108.75, whereas the D-arabitol synthesis rate remained low, with a volumetric productivity of 0.7 g/(L·h). This indicated that cell growth dominated and product synthesis was not yet the primary metabolic objective.

Phase II (30-135 h): Product-synthesis phase. When residual glucose concentration declined below 85 g/L, the feeding program was initiated to maintain glucose concentration at approximately 230 g/L. Cell growth decelerated during this phase, with $OD_{600}$ increasing to 190.36, while D-arabitol accumulated significantly to 129.54 g/L at a volumetric productivity of 0.96 g/(L·h). The metabolic flux was clearly directed toward D-arabitol biosynthesis.

Phase III (135-172 h): Accelerated product synthesis. Following the cessation of glucose feeding, a clear metabolic decoupling between cell growth and product synthesis emerged. Cell growth ceased, leading to accumulation of intracellular ATP and NAD(P)H reserves. The redirected metabolic flux reallocated PPP intermediates, such as ribulose-5-phosphate and xylulose-5-phosphate, away from growth-associated biosynthetic pathways (like nucleotide and amino acid synthesis) toward D-arabitol synthesis. Supported by the sustained intracellular ATP and NAD(P)H levels, this metabolic reconfiguration enabled massive product accumulation, achieving a volumetric productivity of 1.28 g/(L·h) and a final D-arabitol concentration of 220.85 g/L.

Comparative analysis with previous studies on D-arabitol production by osmotolerant yeasts revealed that this work achieved significant advances in both final concentration and volumetric productivity (Table.1). The D-arabitol concentration represents the highest reported in the literature for glucose-based fermentation, demonstrating the effectiveness of the strain-development strategy based on *W. anomalus* K955 and confirming the substantial industrial potential of mutant A37 for D-arabitol production.

**Table.1 Production of D-arabitol by different microorganisms**

| Strain | Substrate | D-arabitol (g/L) | Volumetric productivity (g/(L·h)) | References |
|---|---|---|---|---|
| *Metschnikowia reukaufii* AJ14787 | Glucose | 206.00 | 1.690 | Nozaki et al., 2003 |
| *Zygosaccharomyces rouxiii* NRRL 27624 | Glucose | 83.40 | 0.348 | Saha et al., 2007 |
| *Kodamaea ohmeri* NH-9 | Glucose | 81.20 | 1.128 | Zhu et al., 2010 |
| *Debaryomyces hansenii* NRRL Y-7483 | Glycerol | 40.00 | 0.330 | Koganti and Ju, 2013 |
| *Zygosaccharomyces rouxiiii* JM-C46 | Glucose | 93.48 | 1.143 | Qi et al., 2015 |
| *Rhodosporidium toruloides* IFO0880 | Xylose | 49.00 | 0.200 | Jagtap and Rao, 2018 |
| *Candida parapsilosis* A6 | Glucose | 54.96 | 0.760 | Zheng et al., 2020 |
| *Wickerhamomyces anomalus* WC 1501 | Glycerol | 18.00 | 0.130 | Amaretti et al., 2020 |
| *Yarrowia lipolytica* ARA9 | Glycerol | 118.50 | 1.100 | Yang et al., 2021 |
| *Metschnikowia reukaufii* CICC 31858 | Glucose | 80.43 | 0.560 | Huang et al., 2022 |
| *Wickerhamomyces anomalus* WC 1501 | Glycerol | 265.00 | 0.820 | Raimondi et al., 2022 |
| *Zygosaccharomyces rouxiii* ZR-5A | Glucose | 149.10 | 1.040 | Li et al., 2023 |
| *Zygosaccharomyces siamensis* kiy1 | Glucose | 101.40 | 0.696 | Iwata et al., 2023 |
| *Zygosaccharomyces rouxiii* ZR-M3 | Glucose | 152.80 | 0.800 | Zhang et al., 2024 |
| *Zygosaccharomyces rouxiii* Gz-5 | Glucose | 133.00 | 0.396 | Iwata et al., 2024 |
| *Zygosaccharomyces rouxiii* ST109 | Glucose | 137.60 | 0.640 | Li et al., 2024 |
| *Wickerhamomyces anomalus* A37 | Glucose | 220.85 | 1.280 | This study |



## 4 Discussion

This study addressed critical bottlenecks in the industrial production of D-arabitol, a high-value bio-based chemical, specifically with regard to strain-performance limitations. Through a systematic approach integrating combinatorial mutagenesis, HTS, and transcriptomic analysis, a superior engineered strain, *W. anomalus* A37, was successfully developed and characterized.

Microbial biosynthesis of D-arabitol is fundamentally constrained by osmotic tolerance and metabolic flux allocation(Kordowska-Wiater, 2015; Ravikumar et al., 2022). Current industrial production relies primarily on natural strains of *Metschnikowia* and *Zygosaccharomyces* species, yet significant room exists for yield and tolerance improvements. While rational genetic engineering enables targeted optimization, random mutagenesis frequently achieves global metabolic rebalancing that is difficult to predict through rational design alone, particularly in non-model yeasts with complex metabolic networks. In this work, we implemented a combinatorial mutagenesis strategy employing low-energy $N^+$ ion implantation and DES, coupled with INT-based HTS. Since D-arabitol synthesis is strongly dependent on reduced power availability, this screening strategy effectively enriched for mutants with enhanced NAD(P)H regeneration capacity. This targeted approach successfully isolated *W. anomalus* strain A37, which achieved 108.69 g/L of D-arabitol in shake flasks, a 22.3% improvement over the wild-type K955.

To validate industrial feasibility, we conducted fed-batch fermentation of A37 in a 3L bioreactor, achieving a final D-arabitol titer of 220.85 g/L with volumetric productivity of 1.28 g/(L·h). Using glucose as the carbon source, this titer represents the highest reported in the literature to date. While *W. anomalus* strains have reportedly achieved 265 g/L using glycerol as a substrate(Raimondi et al., 2022), the glucose-based titer of 220.85 g/L has a more economical substrate and demonstrates exceptional competitiveness. Critically, volumetric productivity, a decisive metric for industrial economic viability, reached 1.28 g/(L·h), exceeding many reported high-performance strains, including the above-mentioned glycerol-fermenting *W. anomalus* strains (0.82 g/(L·h)) (Raimondi et al., 2022) and glucose-fermenting *Yarrowia lipolytica* ARA9 (1.10 g/(L·h))(Yang et al., 2021). Achieving simultaneously high volumetric productivity and elevated product concentration demonstrates the exceptional efficacy of the combinatorial mutagenesis strategy in generating metabolically efficient strains.

Systematic transcriptomic analysis revealed that A37 underwent comprehensive global metabolic reprogramming, characterized by intensified carbon flux through PPP and enhanced ribosome biogenesis. Notably, synergistic upregulation of key PPP genes *zwf, gnd*, and *rpe* was central to this metabolic remodeling. PPP serves dual critical functions: it is the primary source of the precursor D-ribulose-5-phosphate for D-arabitol synthesis and the cellular hub for NAD(P)H generation( Stincone et al., 2015; Jagtap and Rao, 2018; Ge et al., 2020). Enhanced *zwf* and *gnd* expression intensified oxidative PPP flux, supplying abundant NADPH cofactors for the reductive reaction catalyzed by aldose reductase(Ingram and Wood, 1965). Concurrently, *rpe* upregulation facilitated non-oxidative PPP isomerization reactions, maintaining optimal precursor equilibrium(Ingram and Wood, 1965). This metabolic homeostasis, featuring both high precursor availability and abundant reducing power, constitutes the molecular foundation for the high D-arabitol production of A37. Notably, this metabolic network remodeling induced by combinatorial mutagenesis parallels the effects of rationally overexpressing rate-limiting PPP enzymes(Povelainen and Miasnikov, 2006), demonstrating that non-transgenic approaches can achieve adaptive evolution equivalent to that produced by targeted metabolic engineering.

Beyond carbon-metabolism remodeling, A37 exhibited comprehensive upregulation of genes governing ribosome biogenesis and translation. Ribosomal protein abundance directly determines cellular translational capacity and growth rate(Metzl-Raz et al., 2017; Björkeroth et al., 2020). Enhanced protein synthesis capability in A37 enabled rapid biosynthesis and sustained high-level expression of metabolic enzymes even under the elevated osmotic pressure characteristic of the late fermentation stage, thereby maintaining vigorous metabolic flux. The robust ribosomal infrastructure and elevated translational capacity enable A37 to preserve vigorous metabolic activity and cellular maintenance mechanisms even during the late stationary phase, accounting for the prolonged product-synthesis phase observed in the fed-batch fermentation profile.

Although strain A37 demonstrated exceptional performance in the 3L bioreactor, several engineering challenges must be addressed for industrial scale-up. First, oxygen-transfer efficiency (OTE) represents a primary bottleneck. In large-scale fermenters, maintaining a consistent 25% dissolved oxygen (DO) level becomes energetically demanding due to increased hydrostatic pressure and mixing dead zones. A decline in the oxygen-transfer rate (OTR) could potentially shift the metabolic flux of A37 from the PPP pathway toward ethanol or glycerol synthesis. Second, heat dissipation is critical during high-intensity fermentation. D-arabitol biosynthesis is an exothermic process; the limited specific surface area of industrial-scale tanks may lead to inadequate cooling and localized overheating, which risks strain inactivation or increased byproduct formation. Furthermore, the precision of the concentrated feeding strategy presents a significant challenge. At scale, the uneven mixing of the highly viscous 900 g/L glucose feed can create transient localized sugar gradients, disrupting metabolic homeostasis. Lastly, the costs associated with maintaining sterility during prolonged, large-scale continuous feeding operations would increase exponentially. In summary, this work not only developed a high-performance strain with industrial application potential but, more significantly, established an

efficient paradigm for strain engineering. By integrating combinatorial mutagenesis with transcriptomic analysis, this framework enables rapid generation of superior strains while providing mechanistic insights into their metabolic basis. This integrated strategy offers significant reference value for developing optimized strains for diverse microbial manufacturing processes.

**Data availability statement**

Original data generated in this study are available from the corresponding author on reasonable request.

**Acknowledgments**

This work was supported by the National Natural Science Foundation of China (No. 22278362), the Public Welfare Project of Zhejiang Provincial Science and Technology Department (No. LGG21B06005) and Quzhou Major Science and Technology Research Projects (No. 2025Z006).

**Author contributions**

All authors contributed to the study conception and design. Mianbin WU designed the experiments. Jikun XIA performed the experiments, analyzed the data and drafted the manuscript. Jialin ZHU performed material preparation. Xudong XU performed data collection. Lvyang LIN performed the bioreactor fermentation. Jianping LIN and Lidan YE participated in experimental supervision, data analysis, and manuscript revision. All authors read and approved the final manuscript.

**Compliance with ethics guidelines**

Jikun XIA, Jialin ZHU, Xudong XU, Lvyang LIN, Jianping LIN, Lidan YE and Mianbin WU declare that they have no conflict of interest. This article does not contain any studies with human or animal subjects performed by any of the authors.

**Declaration on the use of generative AI tools**

During the preparation of this work, the authors used Gemini to improve language and readability. After using this tool, the authors reviewed and edited the content as needed and take full responsibility for the content of the publication.

# References


Ahmed, Z. (2001). The properties of *candida famata* r28 for d-arabitol production from d-glucose. *Journal of Biological Sciences*, *1*(11), 1005. https://doi.org/10.3923/jbs.2001.1005.1008.

Amaretti, A., Russoa, B., Raimondia, S., Leonardia, A., Focaa, G., Muccib, A., Rossi, M. (2020). Potential of *wickerhamomyces anomalus* in glycerol valorization. *Chemical Engineering Transactions*. https://doi.org/https://doi.org/10.3303/cet2079004.

Björkeroth, J., Campbell, K., Malina, C., Yu, R., Di Bartolomeo, F., & Nielsen, J. (2020). Proteome reallocation from amino acid biosynthesis to ribosomes enables yeast to grow faster in rich media. *Proceedings of the National Academy of Sciences of the United States of America*, *117*(35), 21804-21812. https://doi.org/10.1073/pnas.1921890117.

Blomberg, A., & Adler, L. (1992). Physiology of osmotolerance in fungi. *Advances in Microbial Physiology*, *33*, 145-212. https://doi.org/ 10.1016/s0065-2911(08)60217-9.

Deng, Y., Luo, X., Wang, H., Li, S., Liang, J., & Pang, Z. (2024). Xylitol fermentation characteristics with a newly isolated yeast *wickerhamomyces anomalus* WA. *Fungal Biology*, *128*(2), 1657-1663. https://doi.org/https://doi.org/10.1016/j.funbio.2024.01.004.

Fernandes, N. A. T., Rose, A. L., Simões, L. A., & Dias, D. R. (2023). Chemical and biological evaluation of biosurfactant fractions from *wickerhamomyces anomalus* CCMA 0358. *Applied Microbiology and Biotechnology*, *107*(24), 7621-7633. https://doi.org/10.1007/s00253-023-12811-x.

Ge, T., Yang, J., Zhou, S., Wang, Y., Li, Y., & Tong, X. (2020). The role of the pentose phosphate pathway in diabetes and cancer. *Frontiers in Endocrinology*, *11*, 365. https://doi.org/10.3389/fendo.2020.00365.

Huang, J., An, Y., Zabed, H. M., Ravikumar, Y., Zhao, M., Yun, J., Qi, X. (2022). Enhanced biosynthesis of d-arabitol by *metschnikowia reukaufii* through optimizing medium composition and fermentation conditions. *Applied Biochemistry and Biotechnology*, *194*(7), 3119-3135. https://doi.org/10.1007/S12010-022-03910-Y.

Huyben, D., Nyman, A., Vidaković, A., Passoth, V., Moccia, R., Kiessling, A., Lundh, T. R. (2017). Effects of dietary inclusion of the yeasts *saccharomyces cerevisiae* and *wickerhamomyces anomalus* on gut microbiota of rainbow trout. *Aquaculture*, *473*, 528-537. https://doi.org/10.1016/j.aquaculture.2017.03.024.

Ingram, J. M., & Wood, W. A. (1965). Enzymatic basis for d-arabitol production by *saccharomyces rouxii*. *Journal of Bacteriology*, *89*(5), 1186-1194. https://doi.org/10.1128/jb.89.5.1186-1194.1965.

Iwata, K., Kanokozawa, R., Iwata, A., Maeda, M., Maehashi, K., & Yoshikawa, J. (2024). D-arabitol production by a high arabitol-producing yeast, *zygosaccharomyces sp.* Gz-5 isolated from miso. *Bioscience, Biotechnology, and Biochemistry*. https://doi.org/10.1093/BBB/ZBAE075.

Iwata, K., Maeda, M., Kashiwagi, Y., Maehashi, K., & Yoshikawa, J. (2023). Isolation of *zygosaccharomyces siamensis* kiy1 as a novel arabitol-producing yeast and its arabitol production. *AMB Express*, *13*(1). https://doi.org/10.1186/s13568-023-01581-4.

Jagtap, S. S., & Rao, C. V. (2018). Production of d-arabitol from d-xylose by the oleaginous yeast *rhodosporidium toruloides* IFO0880. *Applied Microbiology and Biotechnology*, *102*(1), 143-151. https://doi.org/10.1007/s00253-017-8581-1.

Koganti, S., Kuo, T. M., Kurtzman, C. P., Smith, N., & Ju, L. K. (2010). Production of arabitol from glycerol: strain screening and study of factors affecting production yield. *Applied Microbiology and Biotechnology*, *90*(1), 257-267. https://doi.org/10.1007/s00253-010-3015-3.

Koganti, S., & Ju, L. K. (2013). *Debaryomyces hansenii* fermentation for arabitol production. *Biochemical Engineering Journal*, *79*, 112-119. https://doi.org/https://doi.org/10.1016/j.bej.2013.07.014.

Kordowska-Wiater, M. (2015). Production of arabitol by yeasts: current status and future prospects. *Journal of Applied Microbiology*, *119*(2), 303-314. https://doi.org/10.1111/jam.12807.

Kosugi, M., Miyake, H., Yamakawa, H., Shibata, Y., Miyazawa, A., Sugimura, T., Kashino, Y. (2013). Arabitol provided by lichenous fungi enhances ability to dissipate excess light energy in a symbiotic green alga under desiccation. *Plant and Cell Physiology*, *54*(8), 1316-1325. https://doi.org/10.1093/pcp/pct079.

Kurtzman, C. P. (2011). Phylogeny of the ascomycetous yeasts and the renaming of pichia anomala to *wickerhamomyces anomalus*. *Antonie Van Leeuwenhoek International Journal of General and Molecular Microbiology*, *99*(1), 13-23.

Li, X., Zabed, H. M., Yun, J., Zhang, Y., Zhao, M., Zhang, C., Qi, X. (2024). Sustainable bio-manufacturing of d-arabitol through combinatorial engineering of *zygosaccharomyces rouxii*, bioprocess optimization and downstream separation. *Bioresource Technology*, *393*, 130162. https://doi.org/10.1016/J.BIORTECH.2023.130162.

Li, X., Zhang, Y., Zabed, H. M., Yun, J., Zhang, G., Zhao, M., Qi, X. (2023). High-level production of d-arabitol by

*zygosaccharomyces rouxii* from glucose: metabolic engineering and process optimization. *Bioresource Technology*, *367*. https://doi.org/10.1016/j.biortech.2022.128251.

Ma, Y., Sun, Z., Zeng, Y., Hu, P., Sun, W., Liu, Y., Tang, Z. (2021). Isolation, identification and function of *pichia anomala* AR2016 and its effects on the growth and health of weaned pigs. *Animals*, *11*(4), 1179. https://doi.org/10.3390/ani11041179.

Mackay, P., Ynddal, L., Andersen, J. V., & McCormack, J. G. (2003). Pharmacokinetics and anti-hyperglycaemic efficacy of a novel inhibitor of glycogen phosphorylase, 1,4-dideoxy-1,4-imino-d- arabinitol, in glucagon-challenged rats and dogs and in diabetic ob/ob mice. *Diabetes Obesity & Metabolism*, *5*(6), 397-407. https://doi.org/10.1046/j.1463-1326.2003.00293.x.

Mayer, K. M., & Arnold, F. H. (2002). A colorimetric assay to quantify dehydrogenase activity in crude cell lysates. *SLAS Discovery*, *7*(2), 135-140. https://doi.org/https://doi.org/10.1177/108705710200700206.

Metzl-Raz, E., Kafri, M., Yaakov, G., Soifer, I., Gurvich, Y., & Barkai, N. (2017). Principles of cellular resource allocation revealed by condition-dependent proteome profiling. *Elife*, *6*. https://doi.org/10.7554/eLife.28034.

Mo, E. K., Kang, H. J., Lee, C. T., Xu, B. J., Kim, J. H., Wang, Q. J., Sung, C. K. (2003). Identification of phenylethyl alcohol and other volatile flavor compounds from yeasts, *pichia farinosa* SKM-l, *pichia anomala* SKM-t, and *galactomyces geotrichum* SJM-59. *Journal of Microbiology and Biotechnology*, *13*(5), 800-808.

Nozaki, H., Suzuki, S. I., Tsuyoshi, N., & Yokozeki, K. (2003). Production of d-arabitol by *metschnikowia reukaufii* AJ14787. *Bioscience, Biotechnology, and Biochemistry*, *67*(9), 1923-1929. https://doi.org/10.1271/bbb.67.1923.

Padilla, B., Gil, J. V., & Manzanares, P. (2018). Challenges of the non-conventional yeast *wickerhamomyces anomalus* in winemaking. *Fermentation-Basel*, *4*(3), 68. https://doi.org/10.3390/fermentation4030068.

Povelainen, M., & Miasnikov, A. N. (2006). Production of d-arabitol by a metabolic engineered strain of *bacillus subtilis*. *Biotechnology Journal*, *1*(2), 214-219. https://doi.org/https://doi.org/10.1002/biot.200500035.

Qi, X., Luo, Y., Wang, X., Zhu, J., Lin, J., Zhang, H., Sun, W. (2015). Enhanced d-arabitol production by *zygosaccharomyces rouxii* JM-c46: isolation of strains and process of repeated-batch fermentation. *Journal of Industrial Microbiology & Biotechnology*, *42*(5), 807-812. https://doi.org/10.1007/s10295-015-1603-z.

Raimondi, S., Foca, G., Ulrici, A., Destro, L., Leonardi, A., Buzzi, R., Amaretti, A. (2022). Improved fed-batch processes with *wickerhamomyces anomalus* WC 1501 for the production of d-arabitol from pure glycerol. *Microbial Cell Factories*, *21*(1), 179. https://doi.org/10.1186/S12934-022-01898-Y.

Ranieri, R., Candeliere, F., Sola, L., Leonardi, A., Rossi, M., Amaretti, A., & Raimondi, S. (2024). Production of arabitol from glycerol by immobilized cells of *wickerhamomyces anomalus* WC 1501. *Frontiers in Bioengineering and Biotechnology*, *12*, 1375937. https://doi.org/10.3389/fbioe.2024.1375937.

Ravikumar, Y., Razack, S. A., Ponpandian, L. N., Zhang, G., Yun, J., Huang, J., Qi, X. (2022). Microbial hosts for production of d-arabitol: current state-of-art and future prospects. *Trends in Food Science & Technology*, *120*, 100-110. https://doi.org/https://doi.org/10.1016/j.tifs.2021.12.029.

Saha, B. C., Sakakibara, Y., & Cotta, M. A. (2007). Production of d-arabitol by a newly isolated *zygosaccharomyces rouxii*. *Journal of Industrial Microbiology & Biotechnology*, *34*(7), 519-523. https://doi.org/10.1007/s10295-007-0211-y.

Saha, S., Bridges, S., Magbanua, Z. V., & Peterson, D. G. (2008). Empirical comparison of ab initio repeat finding programs. *Nucleic Acids Research*, *36*(7), 2284-2294. https://doi.org/10.1093/nar/gkn064.

Sánchez-Fresneda, R., Guirao-Abad, J. P., Argüelles, A., González-Párraga, P., Valentín, E., & Argüelles, J. C. (2013). Specific stress-induced storage of trehalose, glycerol and d-arabitol in response to oxidative and osmotic stress in *candida albicans*. *Biochemical and Biophysical Research Communications*, *430*(4), 1334-1339. https://doi.org/10.1016/j.bbrc.2012.10.118.

Shi, K., Gao, Z., Shi, T., Song, P., Ren, L., Huang, H., & Ji, X. (2017). Reactive oxygen species-mediated cellular stress response and lipid accumulation in oleaginous microorganisms: the state of the art and future perspectives. *Frontiers in Microbiology*, *8*, 793. https://doi.org/10.3389/fmicb.2017.00793.

Song, E., Lee, K., & Kim, J. (2022). Tetrazolium-based visually indicating bacteria sensor for colorimetric detection of point of contamination. *ACS Applied Materials & Interfaces*, *14*(33), 38153-38161. https://doi.org/10.1021/acsami.2c08613.

Stincone, A., Prigione, A., Cramer, T., Wamelink, M. M. C., Campbell, K., Cheung, E., Ralser, M. (2015). The return of metabolism: biochemistry and physiology of the pentose phosphate pathway. *Biological Reviews*, *90*(3), 927-963. https://doi.org/https://doi.org/10.1111/brv.12140.

Thammaket, J., Srimongkol, P., Ekkaphan, P., Thitiprasert, S., Niyomsin, S., Chaisuwan, T., Thongchul, N. (2024). Isolation, screening, and characterization of the newly isolated osmotolerant yeast *wickerhamomyces anomalus* BKK11-4 for the coproduction of glycerol and arabitol. *Brazilian Journal of Microbiology*, *55*(3), 2149-2167. https://doi.org/10.1007/s42770-024-01383-1.

Walker, G. M. (2011). *Pichia anomala*: cell physiology and biotechnology relative to other yeasts. *Antonie Van Leeuwenhoek International Journal of General and Molecular Microbiology*, *99*(1), 25-34. https://doi.org/10.1007/s10482-010-9491-8.

Wang, W., Fan, G., Li, X., Fu, Z., Liang, X., & Sun, B. (2020). Application of *wickerhamomyces anomalus* in simulated solid-state fermentation for baijiu production: changes of microbial community structure and flavor metabolism. *Frontiers in Microbiology*, *11*, 598758. https://doi.org/10.3389/fmicb.2020.598758.

Yan, S., Wang, S., Zhai, Z., & Chen, X. (2017). Mutation breeding of salt-tolerant and ethanol-producing strain *s. Cerevisiae* h058 by low-energy ion implantation. *Advance Journal of Food Science and Technology*, *6*(7), 941-946. https://doi.org/10.19026/ajfst.6.136.

Yang, L., Kong, W., Yang, W., Li, D., Zhao, S., Wu, Y., & Zheng, S. (2021). High d-arabitol production with osmotic pressure control fed-batch fermentation by *yarrowia lipolytica* and proteomic analysis under nitrogen source perturbation. *Enzyme and Microbial Technology*, *152*, 109936. https://doi.org/https://doi.org/10.1016/j.enzmictec.2021.109936.

Zha, Y., Hossain, A. H., Tobola, F., Sedee, N., Havekes, M., & Punt, P. J. (2013). *Pichia anomala* 29x: a resistant strain for lignocellulosic biomass hydrolysate fermentation. *Fems Yeast Research*, *13*(7), 609-617. https://doi.org/ 10.1111/1567-1364.12062.

Zhang, G., Zabed, H. M., Zhang, Y., Li, J., Yun, J., & Qi, X. (2024). Random mutagenesis and transcriptomics-guided rational engineering in *zygosaccharomyces rouxii* for elevating d-arabitol biosynthesis. *Bioresource Technology*, *400*. https://doi.org/10.1016/j.biortech.2024.130685.

Zheng, S., Jiang, B., Zhang, T., & Chen, J. (2020). Combined mutagenesis and metabolic regulation to enhance d-arabitol production from *candida parapsilosis*. *Journal of Industrial Microbiology & Biotechnology*. https://doi.org/10.1007/s10295-020-02278-4.

Zhu, H., Xu, H., Dai, X., Zhang, Y., Ying, H., & Ouyang, P. (2010). Production of d-arabitol by a newly isolated *kodamaea ohmeri*. *Bioprocess and Biosystems Engineering*, *33*(5), 565-571. https://doi.org/10.1007/s00449-009-0378-x.



**Supplementary information**

Figs. S1–S11; Tables S1 and S2